

## All-epitaxial fabrication of thick, orientation-patterned GaAs films for nonlinear optical frequency conversion

L. A. Eyres,<sup>a)</sup> P. J. Tourreau,<sup>b)</sup> T. J. Pinguet, C. B. Ebert,<sup>c)</sup> J. S. Harris, and M. M. Fejer  
*Center for Nonlinear Optical Materials, Stanford University, Stanford, California 94305-4090*

L. Becouarn,<sup>d)</sup> B. Gerard, and E. Lallier  
*Laboratoire Central de Recherches, THALES, Domaine de Corbeville-91404 Orsay Cedex, France*

(Received 19 February 2001; accepted for publication 12 June 2001)

Orientation-patterned GaAs (OPGaAs) films of 200  $\mu\text{m}$  thickness have been grown by hydride vapor phase epitaxy (HVPE) on an orientation-patterned template fabricated by molecular beam epitaxy (MBE). Fabrication of the templates utilized only MBE and chemical etching, taking advantage of GaAs/Ge/GaAs heteroepitaxy to control the crystal orientation of the top GaAs film relative to the substrate. Antiphase domain boundaries were observed to propagate vertically under HVPE growth conditions so that the domain duty cycle was preserved through the thick GaAs for all domain periods attempted. Quasiphase-matched frequency doubling of a  $\text{CO}_2$  laser was demonstrated with the beam confocally focused through a 4.6 mm long OPGaAs film. © 2001 American Institute of Physics. [DOI: 10.1063/1.1389326]

Though GaAs has many advantageous characteristics for nonlinear optical frequency conversion including a large nonlinear susceptibility ( $d_{14} \geq 90 \text{ pm/V}$ ), transparency from 1.0  $\mu\text{m}$  to beyond 12  $\mu\text{m}$ , and a high thermal conductivity (46 W/mK), its isotropic nature precludes birefringent phasematching. GaAs and other potentially useful zincblende semiconductors like ZnSe are not ferroelectric and no techniques analogous to electric field poling in  $\text{LiNbO}_3$  exist for inducing a quasi-phase-matching (QPM)<sup>1</sup> domain grating in an already grown crystal. This QPM problem was solved first by the stack of plates approach<sup>2</sup> and made practical with the addition of wafer bonding.<sup>3,4</sup> This approach proved successful and capable of generating crystals of large aperture, but remains limited, as it is a serial fabrication process. In addition, fabricating very short period gratings by these techniques is extremely challenging. First order QPM of parametric processes pumped at  $\lambda = 1.064$ , 1.55, and 2.1  $\mu\text{m}$  require domain periods around  $\Lambda = 9$ , 27, and 60  $\mu\text{m}$ , respectively, where the period  $\Lambda$  and coherence length  $l_c$  are defined as

$$\Lambda = 2l_c = \left( \frac{n_p}{\lambda_p} - \frac{n_s}{\lambda_s} - \frac{n_i}{\lambda_i} \right)^{-1} \quad (1)$$

using the wavelengths  $\lambda$  and refractive indices  $n$  of the pump, signal, and idler waves.

Techniques have also been developed which make possible the epitaxial growth of orientation-patterned semiconductor films using either wafer-bonded templates<sup>5</sup> or all-epitaxially fabricated templates.<sup>6,7</sup> Work to date has focused on waveguide devices, but the same techniques can produce

orientation templates for growth of films thick enough for focusing gaussian beams through the film aperture. Bulk focusing through thick apertures eliminates the limitations on power handling that result from the small apertures of waveguide devices. Beaucarn *et al.*<sup>8</sup> have demonstrated growth of GaAs orientation-patterned layers on polished wafer-bonded stacks of plates. Combining epitaxial template technology and thick GaAs growth enables a more practical approach to fabrication of thick orientation-patterned GaAs films. We report here the fabrication of 200- $\mu\text{m}$ -thick orientation-patterned GaAs (OPGaAs) films and demonstrate the feasibility of growing apertures suitable for bulk frequency conversion with excellent domain quality. We have performed frequency doubling of  $\text{CO}_2$  laser radiation with near theoretical efficiency in these films and observe good optical transmission in the near and mid-IR.

The OPGaAs films are fabricated by a multistep process illustrated in Fig. 1. First, GaAs/Ge/GaAs heteroepitaxy<sup>6</sup> is used to create an inverted or antiphase GaAs layer on a GaAs substrate [Fig. 1(a)], after which this wafer is patterned to create an orientation template [Fig. 1(b)]. This template then undergoes two epitaxial growth steps to produce the thick OPGaAs film [Figs. 1(c) and 1(d)].

More specifically, a 1- $\mu\text{m}$ -thick GaAs/ $\text{Al}_{0.8}\text{Ga}_{0.2}\text{As}$  superlattice buffer terminating in a final 1000  $\text{\AA}$  GaAs layer is grown by molecular beam epitaxy (MBE) on a (100) GaAs wafer misoriented  $4^\circ$  towards (111)B. The superlattice buffer is required to prevent roughening of the wafer surface during growth. A 30  $\text{\AA}$  Ge layer is then grown on top of the GaAs at  $350^\circ\text{C}$ , followed by exposure to an  $\text{As}_2$  prelayer at  $500^\circ$  and growth of a 200  $\text{\AA}$  GaAs layer at  $500^\circ\text{C}$  whose crystallographic orientation is rotated  $90^\circ$  around the [100] direction with respect to the substrate, equivalent to an inversion in the  $\bar{4}3m$  zincblende structure. Finally, a top 500  $\text{\AA}$   $\text{Al}_{0.8}\text{Ga}_{0.2}\text{As}$  layer is grown to protect the underlying GaAs from contamination. All MBE growth was performed using a Varian Gen II MBE system with a valved arsenic cracker. Exposure and development of a photoresist etch mask followed by chemi-

<sup>a)</sup>Electronic mail: eyres@loki.stanford.edu

<sup>b)</sup>Present address: NetTest, 52 Avenue de l'Europe, 78160 Marly Le Roi, France.

<sup>c)</sup>Present address: Wafertech, 5509 N. W. Parker St., Camas, Washington 98607.

<sup>d)</sup>Present address: Alcate Submarine Networks, Route de Villejst, 91625 Nozay Cedex, France

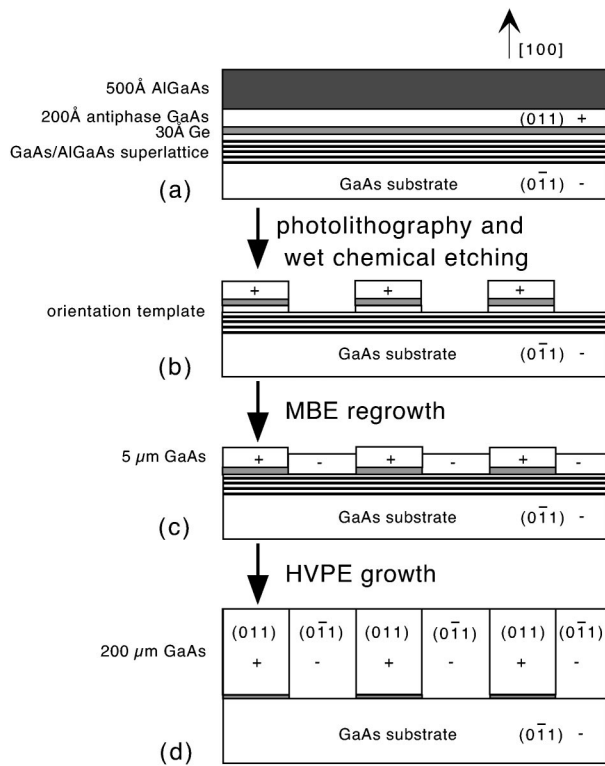


FIG. 1. Fabrication process for thick orientation-patterned GaAs.  $\pm$  indicates both the polarity of the GaAs layers and the sign of the nonlinear susceptibility.

cal etching down to the substrate produces an orientation grating pattern across the wafer surface. Employing a selective etch (citric acid/hydrogen peroxide in a 4:1 ratio),<sup>9</sup> we stop at the top  $\text{Al}_{0.8}\text{Ga}_{0.2}\text{As}$  etch stop layer of the superlattice, after which the top protective  $\text{Al}_{0.8}\text{Ga}_{0.2}\text{As}$  and the etch stop are removed using 1:1  $\text{HCl}/\text{H}_2\text{O}$ . A final brief dip in  $\text{H}_2\text{O}_2$  followed by 1:1  $\text{HCl}:\text{H}_2\text{O}$  was necessary to eliminate aluminum-containing residues which caused large defect densities in regrown films. XPS analysis of the wafer surface before the additional  $\text{H}_2\text{O}_2$  dip revealed enhanced Al and O concentrations which disappeared after additional dipping in  $\text{H}_2\text{O}_2$  and  $\text{HCl}:\text{H}_2\text{O}$ . The patterned orientation template produced by this process [Fig. 1(b)] was then placed back into the MBE system for growth of 5  $\mu\text{m}$  GaAs as a seed layer for subsequent thick GaAs growth.

Hydride vapor phase epitaxy (HVPE) growth was performed using a conventional  $\text{AsH}_3/\text{Ga}+\text{HCl}/\text{H}_2$  transport system. The hot-wall horizontal quartz reactor has two inlets, one for flow of  $\text{HCl}+\text{H}_2$  over the 7N Ga source (providing GaCl) and the other for  $\text{AsH}_3$ ,  $\text{H}_2$  carrier flow, and additional HCl. Total flow is about 1 slm. The temperatures of the Ga source and of the GaAs substrate were 850 and 750  $^\circ\text{C}$  respectively, and the growth occurred at atmospheric pressure. The vertical growth rate was about 10  $\mu\text{m}/\text{h}$ . By varying the vapor phase composition (III/V) ratio between 3 and 10), different stable lateral sidewall facets, either  $\{011\}$  or  $\{111\}$ , have been demonstrated in selective-area-masked stripe growth on (100) surfaces by HVPE.<sup>10</sup> For the present experiments we used the growth conditions suitable for  $\{011\}$  sidewalls, which resulted in vertical antiphase domain boundaries.

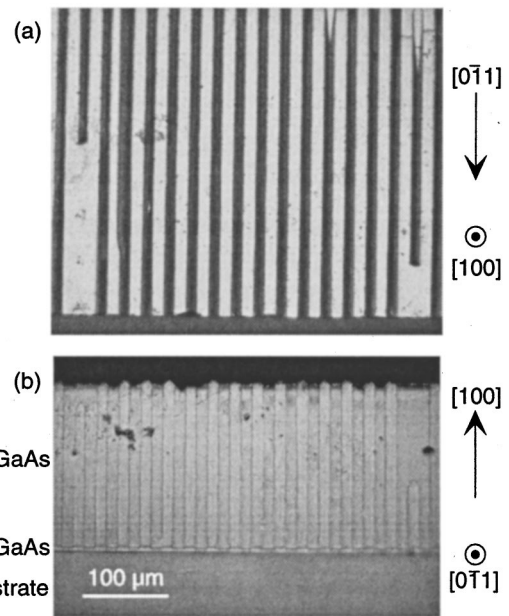


FIG. 2. Top view (a) and stain-etched cross section (b) of 200- $\mu\text{m}$ -thick orientation-patterned GaAs film with 27  $\mu\text{m}$  grating period. Crystal orientations shown are those of the substrate.

cross-section of a 200- $\mu\text{m}$ -thick OPGaAs film with an antiphase domain period of 27  $\mu\text{m}$  (13.5  $\mu\text{m}$  wide domains). The  $\mathbf{k}$  vector of the orientation grating is aligned along the substrate  $[011]$  so the antiphase boundaries (APBs) lie nominally in  $\{011\}$ . The APBs propagate almost exclusively vertically, which preserves the intended domain duty cycle during HPVE growth. With the stable domain propagation observed here, it is reasonable to consider growth of millimeter scale films with similar domain periods. OPGaAs films with gratings aligned in the orthogonal direction (grating  $\mathbf{k}$  vector along the substrate  $[0\bar{1}1]$ ; down the surface atomic steps) are significantly rougher and have lower domain quality. Probably the presence of APBs impedes the propagation of atomic steps across the surface during epitaxial growth and leads to larger corrugations and enhanced probability of domain overgrowth.

Two domains visible in Fig. 2 are interrupted, with the cross section indicating that the domains close over suddenly after growing vertically for much of the film thickness. Examination of the film surface and polished domain cross sections indicates that most of these interruptions originate at the template and increase linearly in length with increasing film thickness. Template defects which could nucleate the interruptions include lithographic defects, oval defects in the MBE-grown films, or contamination resulting from the wet processing.

End facets were polished on  $[011]$  faces of a 4.6 mm long piece of OPGaAs having the 212  $\mu\text{m}$  domain period required for frequency doubling of 10.6  $\mu\text{m}$  radiation. The  $\text{CO}_2$  laser beam was focused to a 50  $\mu\text{m}$  waist using  $\text{BaF}_2$  lenses to make it approximately confocal in the OPGaAs crystal. Using the GaAs refractive index model of Ref. 11, we can calculate the expected sample transmission including two Fresnel reflections to be 51.4%. The maximum measured transmission at 10.5  $\mu\text{m}$  was 50.6%. More accurate attenuation measurements await thicker OPGaAs apertures where

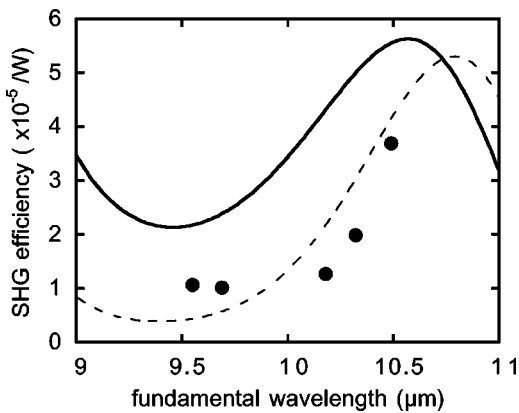


FIG. 3. Internal second harmonic generation efficiency as a function of fundamental wavelength for 4.6 mm long OPGaAs film with 212  $\mu\text{m}$  domain period. Continuous line shows efficiency predicted using refractive index model in Ref. 11; dashed line is theoretical efficiency with additional dispersion shift of  $\Delta n=0.0003$ .

beam clipping at the top air/GaAs interface and highly doped substrate can be eliminated. For second harmonic generation a sapphire plate was used to filter out the fundamental radiation before the second harmonic signal passed through a chopper and onto a pyroelectric detector. The pump radiation was polarized in the plane of the film ( $[1\bar{1}0]$ ), while the generated second harmonic was polarized orthogonal to that direction ( $[001]$ ) as determined by the symmetry of  $d_{14}$ .

Figure 3 shows the measured internal harmonic generation efficiency as a function of fundamental wavelength. The solid line is the tuning predicted with the dispersion relation of Ref. 11. The prediction is quite sensitive to small changes in the dispersion; increasing the dispersion between fundamental and harmonic by  $\Delta n=0.0003$  results in the dashed curve. Note that Ref. 11 reports a rms refractive index deviation between data and model of  $\sim 0.004$ , larger than that necessary to explain the discrepancy between model and data. Extending the measurement to 11  $\mu\text{m}$  would have helped resolve the ambiguity in the dispersion behavior, but the  $\text{CO}_2$  laser available for the experiment could not be tuned beyond 10.5  $\mu\text{m}$ . A lower bound on the effective nonlinear

coefficient can be obtained by assuming the 10.6  $\mu\text{m}$  data point represents the peak of the tuning curve. The result is 47 pm/V. If the dispersion relation used to generate the dashed curve is correct, the best fit value is 55 pm/V. The predicted value assuming  $d_{14}=90$  pm/V is  $d_{\text{eff}}=(2/\pi)*d_{14}=57$  pm/V.

We have demonstrated the growth of thick orientation-patterned GaAs films using all-epitaxial techniques and the frequency doubling of a  $\text{CO}_2$  laser in those films. The antiphase boundaries between regions of opposite orientation propagate vertically under HVPE growth conditions so that the domain duty cycle is preserved. The observed vertical domain propagation with short domain periods offers strong reasons for optimism about fabricating millimeter-scale films with the thin domains required for quasi-phase-matched frequency conversion of mid-IR radiation.

The authors thank Dmitrii Simanovskii and Daniel Palanker for use of their  $\text{CO}_2$  laser and Chris Remen for polishing GaAs samples. This material is based upon work supported by the U.S. Army Research Office under ARO Contract No. DAAH04-96-1-0002. Research was also supported by AFOSR under Grant F49620-99-1-270.

- <sup>1</sup>M. M. Fejer, G. A. Magel, D. H. Jundt, and R. L. Byer, *IEEE J. Quantum Electron.* **28**, 2631 (1992).
- <sup>2</sup>A. Szilagy, A. Hordvik, and H. Schlossberg, *J. Appl. Phys.* **47**, 2025 (1976).
- <sup>3</sup>D. Zheng, L. A. Gordon, Y. S. Wu, R. S. Feigelson, M. M. Fejer, and R. L. Byer, *Opt. Lett.* **23**, 1010 (1998).
- <sup>4</sup>E. Lallier, L. Becouarn, M. Brevignon, and J. Lehoux, *Electron. Lett.* **34**, 1609 (1998).
- <sup>5</sup>S. J. B. Yoo, C. Caneau, R. Bhat, M. A. Koza, A. Rajhel, and N. Antoniadis, *Appl. Phys. Lett.* **68**, 2609 (1996).
- <sup>6</sup>C. B. Ebert, L. A. Eyres, M. M. Fejer, and J. S. Harris, *J. Cryst. Growth* **201/202**, 187 (1999).
- <sup>7</sup>S. Koh, T. Kondo, M. Ebihara, T. Ishiwada, H. Sawada, H. Ichinose, I. Shoji, and R. Ito, *Jpn. J. Appl. Phys., Part 2* **38**, L508 (1999).
- <sup>8</sup>L. Becouarn, B. Gerard, M. Brevignon, J. Lehoux, Y. Gourdel, and E. Lallier, *Electron. Lett.* **34**, 2409 (1998).
- <sup>9</sup>M. Tong, D. G. Balleger, A. Ketterson, E. J. Roan, K. Y. Cheng, and I. Adesida, *J. Electron. Mater.* **21**, 9 (1992).
- <sup>10</sup>E. Gil-Lafon, J. Napierala, D. Castelluci, A. Pimpinelli, R. Cadoret, and B. Gerard, *J. Cryst. Growth* **222**, 482 (2001).
- <sup>11</sup>A. N. Pikhtin and A. D. Yas'kov, *Sov. Phys. Semicond.* **12**, 622 (1978).